NADH, as measured by the pseudo-first-order rate constant k_1 (1.14 s^{-1}), is quite high. Naturally occurring flavoenzymes catalyze the oxidation of NADH with turnover numbers in the range 0.5–35 s^{-1}.[1] Given a suitable electron acceptor to reoxidize the flavin, the turnover number of bacterial 7-acetylflavo-GAPDH could therefore approach that of these biological systems. Unfortunately, electron-accepting dyes that were successfully employed with flavopapain,[29] dichloroindophenol and 3-(4′,5′-dimethylthiazol-2-yl)-2,4-diphenyltetrazolium bromide, are less effective oxidants of reduced flavo-GAPDH than molecular oxygen. It is possible that binding of the bulky dye molecules at the active site is inhibited by bound product. On the other hand, preliminary experiments[30] with cytochrome *c* indicate that this molecule enhances enzyme turnover somewhat over that observed in air-saturated buffer, but it is still not the optimal oxidant. The search for better electron acceptors for reduced 7-acetylflavo-GAPDH therefore continues. Future efforts will also be directed toward improvement of the oxidative and reductive half-reactions by optimizing the electronic structure of the prosthetic flavin moiety and its site of attachment to the enzyme.

Conclusion. Bacterial GAPDH is an excellent template for the construction of stable semisynthetic flavoenzymes. The artificial enzyme we have examined, 7-acetylflavo-GAPDH, is a good catalyst for the oxidation of NADH and NADPH by molecular oxygen, showing rate accelerations at low substrate concentrations 3 orders of magnitude larger than the corresponding nonenzymatic model system. Moreover, the apparent bimolecular rate constant determined at low NADH concentrations is of enzymatic magnitude, as is the pseudo-first-order rate constant for hydride transfer in the enzyme–substrate complex determined by anaerobic stopped-flow procedures. The preference of 7-acetylflavo-GAPDH for hydrophilic substrates was predicted on the basis of a priori considerations of active site geometry and contrasts and complements the specificity for hydrophobic *N*-alkyl-1,4-dihydronicotinamides of the previously prepared flavopapains. Thus, by careful choice of protein template, the substrate specificity of our semisynthetic enzymes can be controlled in a systematic fashion.

Chemical mutation of existing tertiary structures promises to be a general strategy for the construction of artificial enzymes, especially if performed in conjunction with manipulations of the peptide backbone of the template protein. The availability of numerous natural variants makes GAPDH a particularly valuable model template. Our work with the bacterial enzyme has extended our earlier studies with rabbit muscle GAPDH. Using molecular graphics and crystallographic data, we have already been able to understand the differences in substrate specificity and stereoselectivity in the oxidation of dihydronicotinamides by the thermophilic and muscle 7-acetylflavo-GAPDHs in terms of their different quaternary structures. Examination of several other variants will permit a systematic investigation of the relationships between protein structure, catalysis, and regulation. Ultimately, site-directed mutagenesis using recombinant DNA techniques will enable us to construct even more sophisticated semisynthetic catalysts.

Acknowledgment. The partial support of this work by NIH Postdoctoral Fellowship AM-07232 (D.H.) and NSF Grant CHE-8218637 (E.T.K.) is gratefully acknowledged. We thank Desmond Roche for carrying out some preliminary experiments, Dr. Alan Wonacott for providing us with the coordinates of holo-GAPDH from *B. stearothermophilus*, and Drs. Arthur Olson and Alan Schwabacher for helpful discussions.

(29) Radziejewski, C.; Ballou, D. P.; Kaiser, E. T. *J. Am. Chem. Soc.* **1985**, *107*, 3352–3354.
(30) Kokubo, T., unpublished results.

Vibrational Circular Dichroism in the CH Stretching Region of (+)-3(*R*)-Methylcyclohexanone and Chiral Deuteriated Isotopomers

Teresa B. Freedman,* James Kallmerten, Elmer D. Lipp, Daryl A. Young, and Laurence A. Nafie*

Contribution from the Department of Chemistry, Syracuse University, Syracuse, New York 13244-1200. *Received April 13, 1987*

Abstract: The CH stretching Raman, FTIR, and vibrational circular dichroism (VCD) spectra of 3(*R*)-methylcyclohexanone and its chiral *2,2,6,6-d*$_4$, *4,4-d*$_2$, *5,5-d*$_2$ and *methyl-d*$_3$ isotopomers, and the Raman and FTIR spectra of racemic 3-methylcyclohexanone-*3-d*$_1$ are presented and analyzed. Fourier self-deconvolution has been applied to the FTIR spectra to artificially enhance the resolution in order to determine individual band frequencies. Band assignments have been obtained on the basis of the spectral changes occurring due to selective deuteriation and from an analysis of the strong Fermi resonance interactions. The VCD spectral features of the five chiral isotopomers can all be understood in terms of the coupling of pairs of chirally oriented CH oscillators on adjacent carbon atoms and the removal of the degeneracy in the methyl modes.

The utility of vibrational circular dichroism (VCD)[1-4] as a probe of molecular conformation in solution arises in part from the fairly localized nature of many vibrational modes, which thus probe local geometry. Two general mechanisms for VCD intensity have been proposed that relate molecular conformation and the sign of the VCD signal due to localized vibration. The ring current mechanism[1,5,6] accounts for biased or monosignate VCD intensity due to local vibrational motion adjacent to or within a ring closed by covalent or intramolecular hydrogen bonding. Ring current enhancement has been observed for vibrational motion adjacent to

(1) Freedman, T. B.; Nafie, L. A. In *Topics in Stereochemistry*; Eliel, E. L., Wilen, S. H., Eds.; Wiley: New York, 1987; Vol. 17, pp 113–206.
(2) Keiderling, T. A. *Appl. Spectrosc. Rev.* **1981**, *17*, 189.
(3) Nafie, L. A. In *Advances in Infrared and Raman Spectroscopy*; Clark, R. J. M., Hester, R. E., Eds.; Wiley-Heyden: London, 1984; Vol. 11, p 49.
(4) Stephens, P. J.; Lowe, M. A. *Annu. Rev. Phys. Chem.* **1985**, *36*, 213.
(5) Nafie, L. A.; Freedman, T. B. *J. Phys. Chem.* **1986**, *90*, 763.
(6) Freedman, T. B.; Balukjian, G. A.; Nafie, L. A. *J. Am. Chem. Soc.* **1985**, *107*, 6213.

0002-7863/88/1510-0689$01.50/0

a heteroatom in the ring or vibrational motion within the hydrogen bonding interaction and depends on the presence of delocalizable electron density. In this case the magnetic dipole contributions arise from electronic motion that does not perfectly follow the nuclear motion.

The second primary source of VCD intensity is the coupled oscillator mechanism,[7,8] which gives rise to conservative, bisignate VCD couplets due to the in-phase and out-of-phase coupled motion of two chirally oriented, degenerate, or nearly degenerate oscillators. In this case, the electronic motion perfectly follows the nuclear motion, and the magnetic dipole contributions arise from the spatial arrangement of the local oscillating electric dipoles. Coupled oscillator VCD is observed when two strong oscillating dipoles, such as C=O stretches, couple via dipolar interaction, or when two adjacent similar oscillators, such as methylene antisymmetric stretches, couple via the vibrational kinetic and/or potential energy.[1] When several similar, chirally disposed adjacent groups are present in a molecule, more complex coupling patterns are possible, giving rise to positive and negative VCD features that sum to nearly zero intensity over the frequency region of the coupled modes. Such patterns should, in principle, be predicted by the fixed partial charge[9] (FPC) model of VCD, which represents an extension of the coupled oscillator model to all the internal coordinates of a molecule coupled via the potential and kinetic energies.

Three- to six-membered chiral ring molecules have been the focus of numerous VCD studies,[10-20] since the conformations about the CC bonds are restricted by the presence of the ring, and the structures are therefore fairly rigid. In the absence of interacting substituents or heteroatoms in the ring, the CH stretching VCD spectra in these molecules are mostly unbiased, implying that ring current effects are minimal for saturated hydrocarbon rings. Of particular interest are the six-membered-ring molecules. Laux et al.[19,20] have identified the $CH_2CH_2C^*H$ fragment in chiral six-membered-ring compounds as an "inherently dissymmetric chromophore" responsible for the characteristic (+−+) or (−+−) CH stretching VCD pattern that can be correlated with the two ring chair conformations **1** and **2**, respectively. The three VCD bands were assigned[20] to the two antisymmetric CH_2 stretches and the methine stretch of the fragment which are coupled to yield VCD signals of the observed signs via the nondegenerate coupled oscillator mechanism.

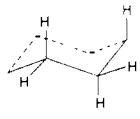

1

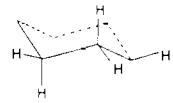

2

(+)-3(*R*)-Methylcyclohexanone (**3**) is the simplest prototype for the molecules containing the $CH_2CH_2C^*H$ fragment. Several studies have reported the CH stretching VCD spectrum and FPC calculations for 3(*R*)-methylcyclohexanone.[10-12] Normal mode calculations were carried out by transferring force constants[10,11] from cyclohexanone[21] and hydrocarbons[22] or by modifying the consistent force field.[12] The calculated VCD spectra in general agreed with the observed (+,−) couplet in the antisymmetric CH_2 stretching region, but the symmetric stretching VCD was not well reproduced in the calculations.

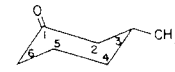

3

There are two major difficulties with the previous VCD studies of 3(*R*)-methylcyclohexanone. The ubiquitous Fermi resonances in hydrocarbons between the symmetric methyl or methylene stretches and the overtones of the methyl deformations or methylene scissors modes have been ignored.[23] The force fields used for the previous FPC calculations are therefore incorrect since these were adjusted to reproduce resonance perturbed observed absorption bands incorrectly assigned to unperturbed fundamentals. Second, the location of the methine stretch is not known, since the C*H methine stretch probably does not have the same force constant as the C(3)H stretch in cyclohexanone (part of a methylene group) as assumed in these earlier studies.

In order to achieve a more accurate interpretation of the CH stretching VCD spectrum of 3(*R*)-methylcyclohexanone, we have prepared both racemic[24] and chiral[25] isotopomers specifically deuteriated at C(2) and C(6), C(3), C(4), C(5), and C(methyl). Our analysis of the FTIR and VCD spectra of these species permits assignment of all the fundamental and Fermi perturbed modes. In addition to FPC calculations, which reproduce the VCD features for the chiral isotopomers, we present an analysis of the VCD spectra in terms of coupled oscillator contributions arising from the mixing of CH stretching modes on adjacent carbon centers.

Experimental Section

(±)-3-Methylcyclohexanone and (+)-3(*R*)-methylcyclohexanone ((+)-MCH), obtained from Aldrich, were freshly distilled prior to use. Racemic and (+)-3(*R*)-[2,2,6,6-$^2H_4$]methylcyclohexanone ((+)-MCH-*2,2,6,6-d*$_4$) were prepared by deuterium exchange from the parent 3-methylcyclohexanone by refluxing with D_2O and potassium carbonate, as described previously for cyclohexanone.[21] The syntheses of (−)-3-(*S*)-[3-$^2H_1$]methylcyclohexanone ((−)-MCH-*3-d*$_1$), (+)-3(*S*)-[4,4-$^2H_2$]-methylcyclohexanone ((+)-MCH-*4,4-d*$_2$), (+)-3(*R*)-[methyl-$^2H_3$]-methylcyclohexanone ((+)-MCH-*methyl-d*$_3$), and (+)-3(*R*)-[5,5-$^2H_2$]-methylcyclohexanone ((+)-MCH-*5,5-d*$_2$) and the corresponding racemic deuteriated isotopomers have been described in detail separately.[24,25] The deuterium incorporation was >95% and completely regiospecific in each case, as determined by NMR, FTIR, and mass spectral analysis. The enantiomeric excesses for the chiral species, determined from the optical rotations, were >90% for (+)-MCH-*5,5-d*$_2$ and (+)-MCH-*2,2,6,6-d*$_4$, ~60% for (+)-MCH-*4,4-d*$_2$ and (+)-MCH-*methyl-d*$_3$, and ~10% for (−)-MCH-*3-d*$_1$.

Spectra were obtained for samples 0.06–0.11 M in CCl_4 in a variable path length cell equipped with CaF_2 or BaF_2 windows. FTIR spectra at 4 cm^{-1} resolution were recorded with a Nicolet 7199 FTIR spectrometer. Fourier self-deconvolution of these spectra in the CH stretching region was performed with the method described by Kauppinen et al.[26] The software was provided by Nicolet Instrument Corp. This technique enhances the resolution of spectra in which bands have Lorentzian contours with bandwidth (full width at half maximum) greater than the instrumental resolution. User input parameters are the bandwidth and a parameter *K* that is related to the factor by which the bandwidth is decreased. A bandwidth of 12 cm^{-1}, estimated from the spectra, and a

(7) Holzwarth, G.; Chabay, I. *J. Chem. Phys.* **1972**, *57*, 1632.
(8) Sugeta, H.; Marcott, C.; Faulkner, T. R.; Overend, J.; Moscowitz, A. *Chem. Phys. Lett.* **1976**, *40*, 397.
(9) Schellman, J. A. *J. Chem. Phys.* **1973**, *58*, 2882; **1974**, *60*, 343.
(10) Polavarapu, P. L.; Nafie, L. A. *J. Chem. Phys.* **1980**, *73*, 1567.
(11) Marcott, C.; Scanlon, K.; Overend, J.; Moscowitz, A. *J. Am. Chem. Soc.* **1981**, *103*, 483.
(12) Singh, R. D.; Keiderling, T. A. *J. Chem. Phys.* **1981**, *74*, 5347.
(13) Singh, R. D.; Keiderling, T. A. *J. Am. Chem. Soc.* **1981**, *103*, 2387.
(14) Annamalai, A.; Keiderling, T. A.; Chickos, J. S. *J. Am. Chem. Soc.* **1984**, *106*, 6254.
(15) Lowe, M. A.; Stephens, P. J.; Segal, G. A. *Chem. Phys. Lett.* **1986**, *123*, 108.
(16) Nafie, L. A.; Keiderling, T. A.; Stephens, P. J. *J. Am. Chem. Soc.* **1976**, *98*, 2715.
(17) Heintz, V. J.; Keiderling, T. A. *J. Am. Chem. Soc.* **1981**, *103*, 2395.
(18) Freedman, T. B.; Paterlini, M. G.; Lee, N.-S.; Nafie, L. A.; Schwab, J. M.; Ray, T. *J. Am. Chem. Soc.* **1987**, *109*, 4727.
(19) Laux, L.; Pultz, V.; Abbate, S.; Havel, H. A.; Overend, J.; Moscowitz, A.; Lightner, D. A. *J. Am. Chem. Soc.* **1982**, *104*, 4276.
(20) Laux, L. Ph.D. Thesis, University of Minnesota, 1982.
(21) Fuhrer, H.; Kartha, V. B.; Krueger, P. J.; Mantsch, H. H.; Jones, R. N. *Chem. Rev.* **1972**, *72*, 439.
(22) Snyder, R. G.; Schachtschneider, J. H. *Spectrochim. Acta* **1965**, *21*, 195.
(23) Lavalley, J. C.; Sheppard, N. *Spectrochim. Acta* **1972**, *28A*, 2091, 845.
(24) Kallmerten, J. *J. Labelled Compd. Radiopharm.* **1983**, *20*, 923.
(25) Kallmerten, J.; Knopp, M.; Durham, L. L.; Holak, I. *J. Labelled Compd. Radiopharm.* **1986**, *23*, 329.
(26) Kauppinen, J. K.; Moffatt, D. J.; Mantsch, H. H.; Cameron, D. G. *Appl. Spectrosc.* **1981**, *35*, 271.

Table I. CH Stretching Frequencies and Assignments for 3-Methylcyclohexanone Isotopomers Based on Fourier Self-Deconvolution of FTIR Spectra

band no.[a]	observed frequencies (cm^{-1}) 3-MCH	3-MCH-*2,2,6,6-d_4*	3-MCH-*3-d_1*	3-MCH-*4,4-d_2*	3-MCH-*5,5-d_2*	3-MCH-*methyl-d_3*	assignment[b]
1	(2962)[c]	2225	(2962)	(2962)	(2961)	2963	$[C(2)H_2, C(6)H_2]^{asym}$
2	(2954)	2218	(2954)	(2955)	(2956)	2955	$[C(2)H_2, C(6)H_2]^{asym}$
3	2962	2962	2962	2962	2961	2216	CH_3^{asym}
4	2954	2954	2954	2955	2956	2208	CH_3^{asym}
5	2940	2941	2941	2941	2208	2945	$C(5)H_2^{asym}$
6	(2935)	2935	(2935)	~2200	(2935)	2937	$C(4)H_2^{asym}$
7	2902	2109[d]	2902	2902	2893	2898	$[C(2)H_2, C(6)H_2]^{sym}$
8	(2918)	2140[d]	(2918)	2918	2915	2918	$[C(2)H_2, C(6)H_2]^{sym}$ } FR
9	2825	2095[d]	2825	2825	2825	2822	$2\delta\ [C(2)H_2, C(6)H_2]$ } FR
10	2927	2927	2926	2927	2928	2138[d]	CH_3^{sym} }
11	2897	2897	2897	2897	(2897)	2116[d]	$2\delta\ (CH_3)$ } FR
12	2869	2870	2870	2870	2872	2066[d]	$2\delta\ (CH_3)$ }
13	(2927)	(2927)	(2927)	(2827)	2198d	2931	$C(5)H_2^{sym}$ }
14	(2869)	(2870)	(2870)	2877	2110d	2865	$2\delta\ (C(5)H_2)$ } FR
15	2910	2906	2909	2189[d]	2908	2909	$C(4)H_2^{sym}$ }
16	2848	2848	2847	2090[d]	2846	2848	$2\delta\ (C(4)H_2)$ } FR
17	2878	(2878)	2125[d]	2886	2878	2878	C(3)H

[a] Band numbers correspond to features in Figure 1. [b] Predominant motion in normal mode, coupled to CH stretches on adjacent carbons (see text). asym = antisymmetric CH_2 or CH_3 stretch; sym = symmetric CH_3 or CH_2 stretch; 2δ = overtone of CH_3 antisymmetric deformation or CH_2 scissors; FR = Fermi resonance diad or triad involving symmetric stretch and deformation overtone(s) in bracket. [c] Frequency in parentheses is estimated from other isotopomers since band is overlapped by more intense feature. [d] Symmetric CD stretches are strongly perturbed by Fermi resonances. Frequencies of most intense observed features are given.

value of 2.5 for K were used to deconvolute each of the spectra.

VCD spectra were recorded at 12 or 7 cm^{-1} resolution with a dispersive VCD spectrometer described previously.[27] For (+)-MCH and (+)-MCH-*2,2,6,6-d_4*, the racemic compound was used for the VCD base line. For (+)-MCH-*4,4-d_2*, (+)-MCH-*5,5-d_2*, and (+)-MCH-*methyl-d_3* racemic (±)-MCH was used for the base line since insufficient racemic isotopomer was available. The low enantiomeric excess and small quantity of (+)-MCH-*3-d_1* available precluded our obtaining accurate VCD data for this isotopomer. The VCD spectra presented here represent the difference of single chart recorder scans for sample and base line.

Raman spectra were obtained for the neat samples as previously described.[28]

Results

The CH stretching absorption spectra obtained for racemic 3-methylcyclohexanone and the five deuteriated isotopomers are shown in Figure 1a–f. Since the CH stretching region contains numerous overlapping bands (twelve fundamentals and at least six overtone and combination bands) we have used Fourier self-deconvolution (FSD)[26] to artificially enhance the resolution in order to identify individual band frequencies. The FSD results obtained from spectra of the racemic species at 4-cm^{-1} resolution are also shown in Figure 1a–f. The FSD frequencies and assignments of bands 1 to 17 are compiled in Table I.

The VCD spectra for five of the isotopomers are shown in Figure 2a–e. These cannot be directly compared to the FSD results in Figure 1 since the frequency axes are linear in wavelength in Figure 2 and linear to wavenumber in Figure 1. Since the concentrations of the deuteriated samples are less certain due to the small quantities of material available, the absorption spectra were scaled to give equal intensity for the C=O stretching band, compared to the parent 3-methylcyclohexanone. The ϵ values in Figure 2b–e are therefore approximate. The VCD intensities have been adjusted to 100% optical purity on the basis of the optical rotations compared to that of pure (+)-MCH. The VCD frequencies, intensities, and assignments are presented in Table II. The VCD spectrum for (+)-MCH-*5,5-d_2* was adjusted to eliminate a badly sloping base line; the VCD intensities for this species are therefore less certain. VCD spectra of (+)-MCH-*3-d_1* were not obtained due to the low optical purity.

Table II. Observed Frequencies and Intensities of VCD Bands in 3(*R*)-Methylcyclohexanone and Deuteriated Isotopomers

isotopomer	freq, cm^{-1}	$10^3\ \Delta\epsilon$, 10^3 $cm^3\ mol^{-1}$	isotopomer	freq, cm^{-1}	$10^3\ \Delta\epsilon$, 10^3 $cm^3\ mol^{-1}$
(+)MCH	2961	−1.5	(+)MCH-*4,4-d_2*	2963	−1.8
	2945	+6.7		2945	+2.9
	2928	−6.8		2918	−2.5
	2909	+3.3		2897	−2.6
	2892	−2.6		2877	+1.5
	2870	−0.5			
(+)MCH-*2,2,6,6-d_4*	2965	−0.4	(+)MCH-*5,5-d_2*	2960	+1.0
	2955	+1.8		2935	+1.5
	2945	+3.0		2907	+0.6
	2932	−8.3		2890	−0.8
	2921	+3.5		2868	−0.9
	2907	+2.2			
	2875	−5.3			
	2847	−0.8			
(+)MCH-*methyl-d_3*	2960	−0.1			
	2948	+1.2			
	2935	−4.6			
	2925	+3.0			
	2915	+4.8			
	2895	−1.4			
	2875	−1.5			

The absorption and VCD spectra in the CD stretching region of (+)-MCH-*2,2,6,6-d_4* are presented in Figure 2f. This was the only isotopomer available in sufficient amount to obtain CD stretching VCD spectra. In order to analyze the Fermi resonance interactions, we compare the FTIR spectra of the six species in the methyl antisymmetric deformation and methylene scissors region in Figure 3 and Table III.

We have also obtained unpolarized Raman spectra of all six racemic isotopomers (Figure 4) and polarized and depolarized Raman spectra of (±)-MCH, all for neat samples. The Raman frequencies and assignments are given in Table IV.

Assignments

A comparison of the Fourier deconvolved spectra in Figure 1a–f allows the assignment of bands to primary contributions from CH motion on individual carbon atoms, since the frequencies of the remaining CH stretches do not shift greatly upon deuteriation at a single carbon center. From the Raman depolarization measurement for (+)-MCH, we find that all the bands from 2930 to 2800 cm^{-1} are strongly polarized, whereas those comprising the ~2955-cm^{-1} Raman feature are depolarized. On the basis

(27) (a) Diem, M.; Gotkin, P. J.; Kupfer, J. M.; Naife, L. A. *J. Am. Chem. Soc.* **1978**, *100*, 5644. (b) Diem, M.; Photos, E.; Khouri, H.; Nafie, L. A. *Ibid.* **1979**, *101*, 6829. (c) Lal, B. B.; Diem, M.; Polavarapu, P. L.; Oboodi, M. R.; Freedman, T. B.; Nafie, L. A. *Ibid.* **1982**, *104*, 3336.

(28) Freedman, T. B.; Kallmerten, J.; Zimba, C. G.; Zuk, W. M.; Nafie, L. A. *J. Am. Chem. Soc.* **1984**, *106*, 1244.

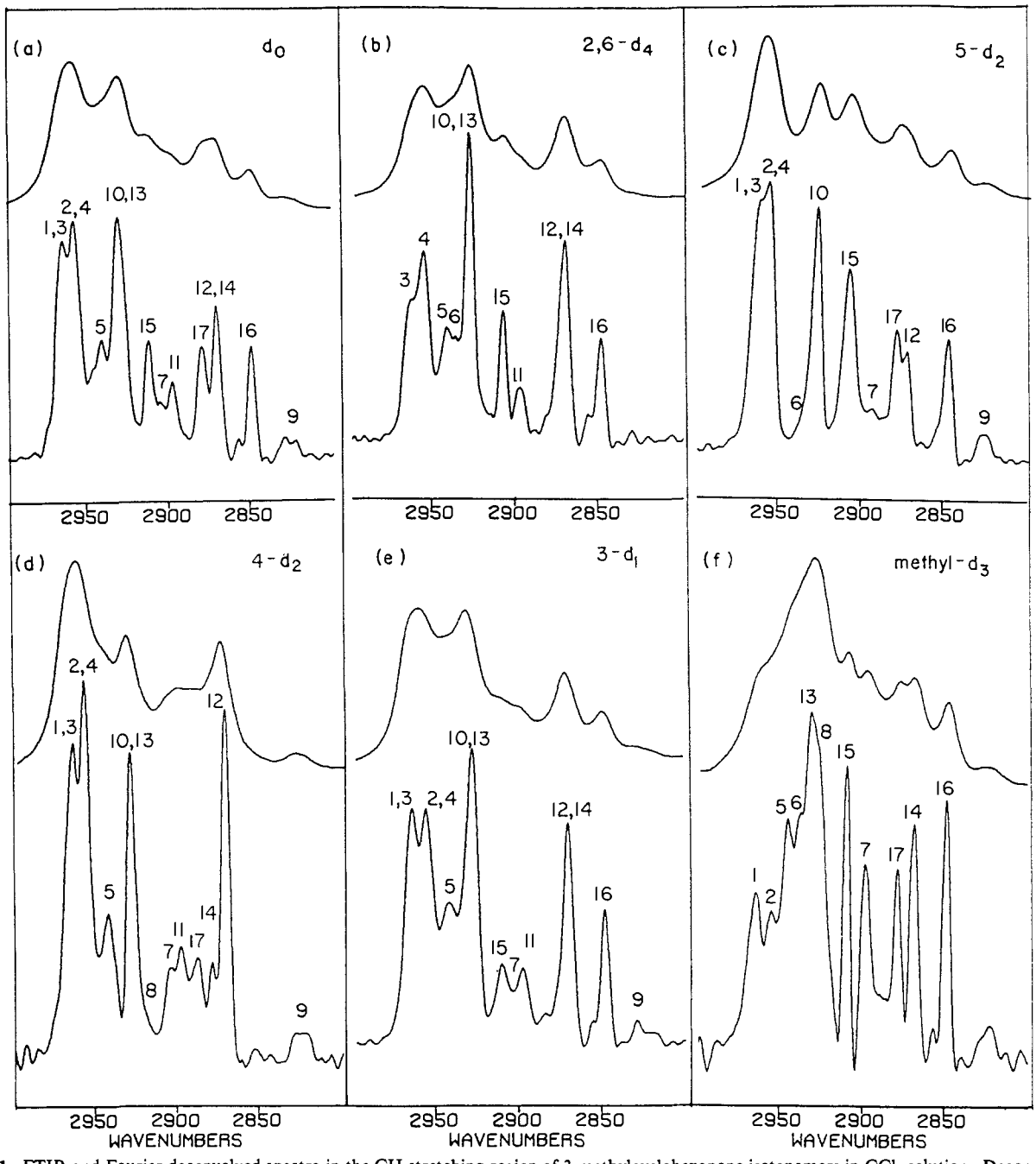

Figure 1. FTIR and Fourier deconvolved spectra in the CH stretching region of 3-methylcyclohexanone isotopomers in CCl_4 solution. Deconvolutions were obtained with 12-cm^{-1} bandwidth and an improvement factor of 2.5. Resolution of FTIR spectra is 4 cm^{-1}. Numbers above bands refer to assignments in Table I. (a) 3-Methylcyclohexanone; (b) 3-methylcyclohexanone-*2,2,6,6-d*$_4$; (c) 3-methylcyclohexanone-*5,5-d*$_2$; (d) 3-methylcyclohexanone-*4,4-d*$_2$; (e) 3-methylcyclohexanone-*3-d*$_1$; (f) 3-methylcyclohexanone-*methyl-d*$_3$.

Table III. Frequencies (cm^{-1}) and Assignments of the Methyl Deformation and Methylene Scissors Modes in 3-Methylcyclohexanone Isotopomers

assignment	MCH	MCH-*2,2,6,6-d*$_4$	MCH-*5,5-d*$_2$	MCH-*4,4-d*$_2$	MCH-*3-d*$_1$	MCH-*methyl-d*$_3$
δ (CH_3^{asym})	1456	1458	1456	1456	1455	
δ ($C(5)H_2$)						1456
δ ($C(4)H_2$)	1447	1445	1450		1448	1447
δ ($C(2)H_2$, $C(6)H_2$)	1426		1425	1429	1426	1426
δ ($C(2)H_2$, $C(6)H_2$)	1421		1420	1420	1421	1421

of these depolarization ratios and the effects of deuteriation as detailed below, we place the antisymmetric modes above 2930 cm^{-1}. The two or more intense bands between 2930 and 2820 cm^{-1} attributable to CH motion at an individual carbon center must thus arise from Fermi resonance interactions involving the symmetric stretches. We consider first the band assignments and will then analyze the Fermi interactions to estimate the unperturbed frequencies of the symmetric stretching modes.

The bands at 2962 (bands 1,2) and 2955 cm^{-1} (bands 3,4) each correspond to a superposition of an antisymmetric methyl stretch and one of the two coupled $C(2)H_2$ and $C(6)H_2$ antisymmetric stretches, as seen by the effects of deuteriation at either the methyl carbon or at C(2) and C(6) (Figures 1a, 1b, and 1f and 4a, 4b, and 4f). The two antisymmetric methyl modes are split in frequency due to the local approximately C_s symmetry of the methyl group in 3-MCH. The weak band at ~2940–2945 cm^{-1} (band

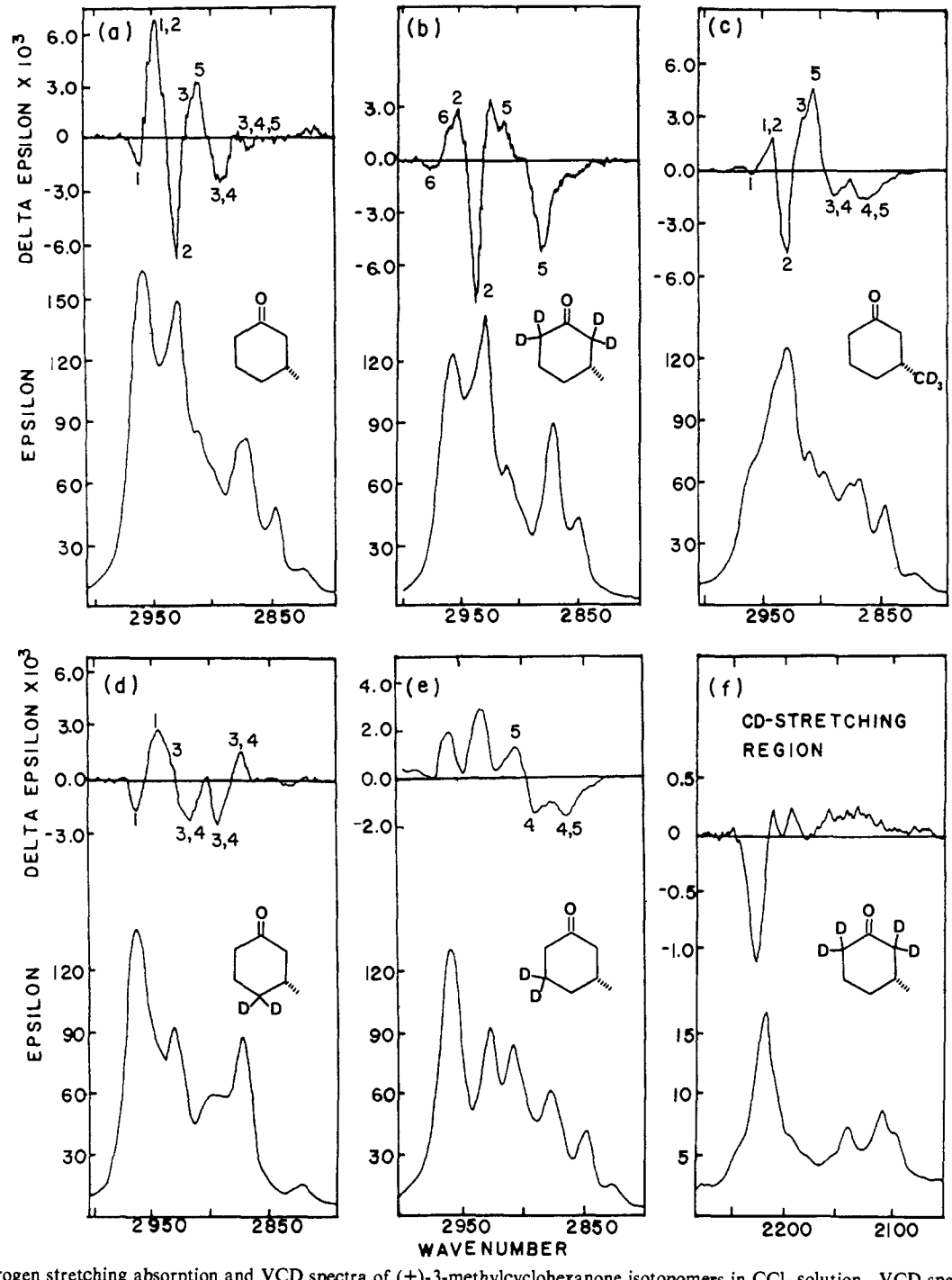

Figure 2. Hydrogen stretching absorption and VCD spectra of (+)-3-methylcyclohexanone isotopomers in CCl_4 solution. VCD spectral resolution: (a–d) 7 cm^{-1}; (e) 12 cm^{-1}; (f) 7 cm^{-1}. Numbers adjacent to VCD bands refer to assignments of VCD couplets in Table VI. (a) (+)-3(*R*)-Methylcyclohexanone; (b) (+)-3(*R*)-methylcyclohexanone-*2,2,6,6-d*$_4$; (c) (+)-3(*R*)-methylcyclohexanone-*methyl-d*$_3$; (d) (+)-3(*S*)-methylcyclohexanone-*4,4-d*$_2$; (e) (+)-3(*R*)-methylcyclohexanone-*5,5-d*$_2$; (f) CD stretching VCD of (+)-3(*R*)-methylcyclohexanone-*2,2,6,6-d*$_4$.

5) is absent in MCH-*5,5-d*$_2$ and is assigned to the C(5)H_2 antisymmetric stretch. The weak ~2935-cm^{-1} feature in the deconvolved spectra of MCH-*2,2,6,6-d*$_4$ and MCH-*methyl-d*$_3$ is absent in MCH-*4,4-d*$_2$. Evidence of a weak absorption feature, although not resolved, is also present at ~2935 cm^{-1} in MCH, MCH-*5,5-d*$_2$, and MCH-*3-d*$_1$. We therefore assign this feature (band 6) to the C(4)–H_2 antisymmetric stretch. As shown from the normal coordinate calculation and VCD interpretation below, for the isotopomers with both C(4)H_2 and C(5)H_2, the 2940- and 2935-cm^{-1} modes involve a mixture of antisymmetric stretching motion at both carbons, although C(5)H_2 motion is dominant in the higher frequency mode and C(4)H_2 motion is dominant in the lower.

Numerous accidental degeneracies occur among the symmetric stretching modes. A pronounced reduction in IR or Raman intensity at both ~2927 and ~2870 cm^{-1} is observed with deuteriation either at C(5) or at the methyl group. From the Fourier deconvolved spectra of MCH-*methyl-d*$_3$ and MCH-*5,5-d*$_2$ we assign bands at ~2930 (band 13) and ~2865 cm^{-1} (band 14) to vibration at C(5)H_2 and bands at ~2927 (band 10) and ~2872 cm^{-1} (band 12) to the methyl group. The nearly equal intensity of the two bands in each isotopomer is indicative of strong Fermi resonances involving the symmetric stretches. The bands at ~2910 (band 15) and 2848 cm^{-1} (band 16) dissappear with deuteriation at C(4) and are assigned to a Fermi diad involving the C(4)H_2 symmetric stretch.

The IR, VCD, and Raman intensity near 2900 cm^{-1} decreases with deuteriation at C(2) and C(6), although a weak absorption and Raman feature at 2897 cm^{-1} remains. We attribute most of the intensity between 2890 and 2902 cm^{-1} (band 7) to the

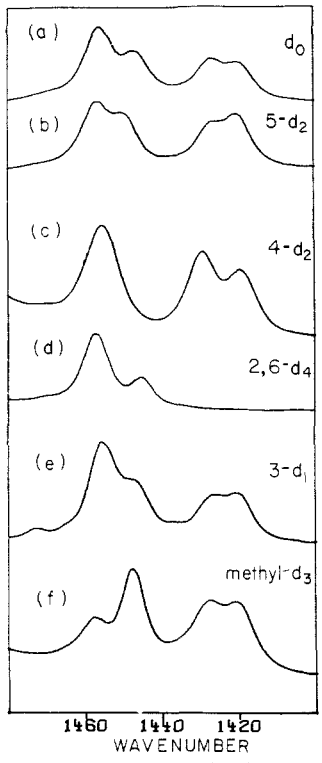

Figure 3. Absorption spectra of 3-methylcyclohexanone isotopomers in the methyl antisymmetric deformation and methylene scissors region, in CCl_4 solution: (a) 3-methylcyclohexanone; (b) 3-methylcyclohexanone-*5,5-d_2*; (c) 3-methylcyclohexanone-*4,4-d_2*; (d) 3-methylcyclohexanone-*2,2,6,6-d_4*; (e) 3-methylcyclohexanone-*3-d_1*; (e) 3-methylcyclohexanone-*methyl-d_3*. Spectral resolution, 4 cm^{-1}.

Table IV. Frequencies (cm^{-1}) of the Major Bands in the Raman Spectra of 3-Methylcyclohexanone Isotopomers in the CH Stretching Region

MCH	MCH-2,2,6,6-d_4	MCH-5,5-d_2	MCH-4,4-d_2	MCH-3-d_1	MCH-methyl-d_3
2957	2952 sh	2958	2959	2955	
2943 sh[a]	2943 sh		2942 sh	2942 sh	2947
2930	2927	2927	2929	2927	2928 sh
2897	2894	2902	2899	2896	2899
2869	2868	2870	2870	2869	2869
2850	2850	2848		2848	2850
2826		2824	2825	2827	2827

[a] Shoulder.

coupled $C(2)H_2$ and $C(6)H_2$ symmetric stretching motion. The weaker 2897-cm^{-1} (band 15) feature apparent in MCH-*2,2,6,6-d_4* can be assigned to the third component of the Fermi resonance triad expected for the methyl group. The second $C(6)H_2$, $C(2)H_2$ symmetric stretch is assigned to the shoulder at 2918 cm^{-1} (band 8) in MCH-*methyl-d_3*. These assignments will be discussed further below.

The methine stretch is assigned at ~2877 cm^{-1} (band 17), since this band disappears in MCH-*3-d_1*, whereas the remaining bands exhibit only slight intensity changes. The 2877-cm^{-1} feature also either shifts to lower frequency or decreases in intensity in MCH-*2,2,6,6-d_4*, indicative of an interaction between C(3)H and $C(2)H_2$ stretches.

In general, for each deuteriated isotopomer, the stretching modes assigned to CH bonds at carbons adjacent to the site of deuteriation show the largest frequency or intensity changes compared with the spectra of the parent MCH. These small but measurable effects are indicative of modes that are largely localized, but which involve some coupling with vibrations at adjacent carbon centers. The frequencies assigned in Table I are those observed in the Fourier deconvolved spectra for each isotopomer. In addition to the major bands assigned above, weaker features are observed in the spectra that correspond to overtones

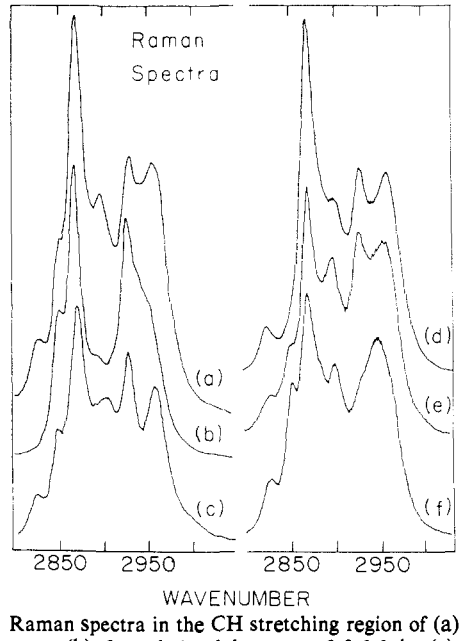

Figure 4. Raman spectra in the CH stretching region of (a) 3-methylcyclohexanone, (b) 3-methylcyclohexanone-*2,2,6,6-d_4*, (c) 3-methylcyclohexanone-*5,5-d_2*, (d) 3-methylcyclohexanone-*4,4-d_2*, (e) 3-methylcyclohexanone-*3-d_1*, (f) 3-methylcyclohexanone-*methyl-d_3* as neat liquids.

and combination bands not readily assignable, with the exception of the band at 2825 cm^{-1} (band 9) attributed to an overtone of a $C(2)H_2 + C(6)H_2$ methyl scissors vibration, since this mode is absent in MCH-*2,2,4,4-d_4*.

In the CD stretching region (2100–2220 cm^{-1}) the Fermi resonance interactions are even more pronounced than for the CH stretching region, resulting in a multitude of bands for each isotopomer that prevents any detailed analysis. The antisymmetric CD_2 and CD_3 stretches, which are the least perturbed by Fermi resonance, occur in the same frequency order as the bands assigned to the corresponding CH stretches. The strong negative VCD band at 2225 cm^{-1} for MCH-*2,2,6,6-d_4* (Figure 2f) corresponds to the higher frequency antisymmetric CD_2 stretch in the deconvolved absorption spectrum.

The frequencies of the antisymmetric methyl deformation and methylene scissors modes are important for understanding the Fermi resonance interactions. From the expanded spectra in this region shown in Figure 3 for the six isotopomers, the individual bands are readily assigned. The two CH_3 antisymmetric deformations occur as an unresolved band at 1456 cm^{-1}. This band is superimposed on the weaker band at 1456 cm^{-1} due to the $C(5)H_2$ scissors mode, as revealed by deuteriation of the methyl group. The $C(4)H_2$ scissors occurs at 1447 cm^{-1}. This mode shifts slightly to higher frequency when the adjacent C(5) methylene is deuteriated and shifts slightly to lower frequency when the C(2) and C(6) methylenes are deuteriated. The $C(2)H_2$ and $C(6)H_2$ scissors motions give rise to bands at 1426 and 1420 cm^{-1} that are in-phase and out-of-phase combinations of the two local scissors modes, since α-CH_2 scissors bands of A′ and A″ symmetry occur in cyclohexanone at these same frequencies.

Fermi Resonance Interactions

When a fundamental vibration (Ψ^0_a) and an overtone of the same symmetry (Ψ^0_b) have nearly the same frequency, the modes can interact through a cubic anharmonic potential energy term W_{ab}, giving rise to perturbed modes[29,30]

$$\Psi_a = a\Psi^0_a + b\Psi^0_b$$

$$\Psi_b = -b\Psi^0_a + a\Psi^0_b$$

with $a^2 + b^2 = 1$. The perturbed modes are separated in energy by $\Delta = (\Delta_0^2 + 4W_{ab}^2)^{1/2}$, where Δ_0 is the separation of the un-

(29) Fermi, E. *Z. Phys.* **1931**, *71*, 250.
(30) Califano, S. *Vibrational States*; Wiley: New York, 1976.

perturbed modes. If the unperturbed overtone has weak or zero intensity, the intensity ratio of the perturbed modes will be

$$\frac{I_a}{I_b} \cong \frac{a^2}{b^2}$$

that is, the intensity of the unperturbed fundamental is distributed between the two perturbed modes. In the VCD spectrum, the rotational strength of the unperturbed fundamental will be similarly divided between the two perturbed levels.

In 3-methylcyclohexanone, the overtones of the methylene scissors and antisymmetric methyl deformation modes are close in frequency to the symmetric methylene and methyl stretches, and strong Fermi resonance occurs. The interactions are far more complex than the two-state Fermi diad, since, although the modes are fairly localized, both the fundamentals and overtones contain contributions from CH motion on more than one carbon. Anharmonic potential terms are possible that result in the interaction of an overtone with two or more fundamentals or a fundamental with two or more overtones. We can, however, unravel some of the interactions, which will enable us to understand the VCD and absorption spectra in more detail.

Due to lowering of symmetry, the methyl group degeneracies are removed in 3-MCH, and the overtones of both of the antisymmetric methyl deformations (unperturbed energy E_2^0 and E_3^0) can interact with the symmetric methyl stretch (unperturbed energy E_1^0) resulting in a Fermi triad with the secular equation[27c]

$$\begin{vmatrix} E_1^\circ - E & W_{12} & W_{13} \\ W_{12} & E_2^\circ - E & 0 \\ W_{13} & 0 & E_3^\circ - E \end{vmatrix} = 0$$

The unresolved antisymmetric methyl deformations occur at 1456 cm^{-1}; the Fermi perturbed methyl modes in the CH stretching region occur at 2927, 2897, and 2872 cm^{-1} (bands 10–12). By assuming that $W_{12} = W_{13}$, and that the anharmonicity[23] for the overtone is ~17 cm^{-1}, and by using the fact that the sum of the frequencies of the unperturbed modes equals the sum of the frequencies for the perturbed modes, we estimate that the frequency of the unperturbed methyl symmetric stretch is 2906 cm^{-1} and that of the unperturbed overtones is 2895 cm^{-1}. These values are quite similar to those for methyl groups in numerous other primarily hydrocarbon environments. For this simplified analysis, the weak mode at 2897 cm^{-1} is found to be the antisymmetric combination of the two overtones, whereas the intense bands at 2927 and ~2870 cm^{-1} are the two linear combinations of the symmetric stretching fundamental and the symmetric combinations of the two overtones.[27c]

For the methylene groups the primary interaction will be between a CH_2 symmetric stretching fundamental and a CH_2 scissors overtone that are localized at the same methylene. As a first approximation, then, we can consider the perturbed modes at ~2930 and ~2870 cm^{-1} (bands 13, 14) that are due largely to $C(5)H_2$ motion, to result from a Fermi resonance between the overtone of the 1456-cm^{-1} $C(5)H_2$ scissors mode and the $C(5)H_2$ symmetric stretch. For a 17-cm^{-1} anharmonicity in the overtone, yielding an unperturbed overtone at 2895 cm^{-1} (2 × 1456 cm^{-1} − 17 cm^{-1}), the unperturbed symmetric stretch is estimated to occur at 2905 cm^{-1} (2930 cm^{-1} + 2870 cm^{-1} − 2895 cm^{-1}). A similar analysis of the perturbed modes at ~2910 and 2849 cm^{-1} (bands 15, 16) and scissors mode at 1447 cm^{-1}, ascribed largely to $C(4)H_2$ motions, results in the frequencies 2882 and 2877 cm^{-1} for the unperturbed fundamental and overtone, respectively.

For the three cases above, the unperturbed interacting modes are separated by 4–10 cm^{-1}, and a strong resonance interaction occurs that results in perturbed modes separated by ~60 cm^{-1}. For both the $C(4)H_2$ and $C(5)H_2$ methylene groups, a value of 31 cm^{-1} for the Fermi coupling constant W_{ab} is found. The band observed at 2825 cm^{-1} (band 9) is associated with the $C(2)H_2$ and $C(6)H_2$ methylenes. Although the unperturbed overtone of the 1421-cm^{-1} scissors is expected at this frequency, no band of comparable intensity corresponding to the unpreturbed overtone of the 1426-cm^{-1} mode is found at ~2835 cm^{-1}, and the observed band at 2825 cm^{-1} has significant intensity compared to the bands assigned to the $C(2)H_2$, $C(6)H_2$ symmetric stretching fundamental near 2900 cm^{-1}. It is more likely that the 2825-cm^{-1} band is part of a Fermi resonant interaction involving the unperturbed overtone of the 1426-cm^{-1} scissors, expected to occur at ~2835 cm^{-1}, and the in-phase $C(2)H_2$, $C(6)H_2$ symmetric stretch. The out-of-phase stretch does not have the proper symmetry to interact with the overtone, and this is the mode observed between 2893 and 2902 cm^{-1} (band 7) in the various isotopomers. We can now ascribe the shoulder observed at ~2918 cm^{-1} (band 8) in the MCH-*methyl-*d_3 isotopomer to the Fermi perturbed $C(2)H_2$, $C(6)H_2$ symmetric stretch. This band is not resolved in the other isotopomers due to the intense CH_3 mode at ~2927 cm^{-1}. In comparing the Fourier deconvolved spectra of MCH and MCH-*2,2,6,6-*d_4 (Figure 1a,b) there is evidence that the bandwidth of the 2927-cm^{-1} feature has decreased in the deuteriated species, also indicative of a contribution from the Fermi perturbed stretch. The VCD spectra are also consistent with a mode near 2918 cm^{-1} due to $C(2)H_2$, $C(6)H_2$ symmetric stretching motion, as will be discussed below.

Although this analysis can only provide approximate frequencies for the unperturbed symmetric stretching fundamentals, for the purposes of describing the normal modes and interpreting the VCD spectra, we find that the correct frequency *order* of the modes is necessary, but not the precise frequency values.

Normal Coordinate and Rotational Strength Calculations

In order to estimate the contributions and determine the phasings of the individual CH oscillations in each stretching mode, we have carried out a normal coordinate analysis for 3-MCH and the deuteriated isotopomers with a modified valence force field. We previously refined the force field determined by Fuhrer et al. for cyclohexanone[21] by adding methyl group force constants[22] and adjusting the diagonal force constants to give close agreement with experiment for the ten lowest frequency modes in all six isotopomers.[28] This force field was used to interpret the Raman optical activity (ROA) spectrum in the skeletal region of (+)-3(*R*)-methylcyclohexanone. For the present study, we have adjusted the diagonal CH stretching and HCH bending force constants and CH,CH stretching interaction force constants to obtain frequencies and mode descriptions for the unperturbed antisymmetric and symmetric CH stretches and antisymmetric methyl deformations and methylene scissors modes assigned by the Fourier deconvolution studies and Fermi resonance analysis described above. Since from the present data there is no way to determine individual force constants for the axial and equatorial CH bonds, these were given equal values for each methylene group. The C(2)H and C(6)H force constants were also kept equal since there is little frequency change for vibrations localized at the C(2) and C(6) methylenes compared to the corresponding modes of cyclohexanone. All three CH bonds of the methyl group were given the same diagonal force constant. The difference in frequency calculated for the two antisymmetric methyl stretches (which agrees closely with the observed splitting) is thus a consequence of the vibrational kinetic energy and the molecular geometry, rather than a result of force constant differences among the methyl CH bonds.

The geometry was transferred from cyclohexanone,[21] substituting a staggered methyl group with standard bond lengths and angles for the equatorial hydrogen at C(3). The chair conformation with an equatorial methyl group has been determined to be the most stable.[12] The VCD features and temperature dependence of the VCD spectra[12] are consistent with this single conformation in solution. The calculations were carried out in Cartesian coordinates in order to readily determine displacement vectors for each nucleus.

The calculated splitting between antisymmetric and symmetric methyl or methylene stretching modes depends on the magnitude of the vicinal CH,CH stretching interaction force constant for the group, a larger (positive) value giving a smaller splitting. The value of this off-diagonal force constant was separately adjusted for each group to reproduce the separation between antisymmetric and unperturbed symmetric stretching modes as estimated by the

Table V. Calculated Frequencies, Rotational Strengths, and Assignments for the CH and CD Stretching Modes of (+)-3(*R*)-Methylcyclohexanone and Deuteriated Isotopomers[a]

assignment[b]	freq, cm^{-1}	*R*(FPC)[c]	*R*(APT)[d]	couplet[e]	assignment[b]	freq, cm^{-1}	*R*(FPC)[c]	*R*(APT)[d]	couplet[e]
	(+)MCH					(+)MCH-*4,4-d*$_2$			
CH_3^{asym}	2962.9	13.2	7.1		CH_3^{asym}	2962.9	4.1	1.8	
$C(2)H_2$, $C(6)H_2^{asym}$	2962.3	−28.4	−22.1	1	$C(2)H_2$, $C(6)H_2^{asym}$	2961.8	−20.7	−19.0	1
$C(2)H_2$, $C(6)H_2^{asym}$	2958.4	−9.2	−7.2	1	$C(2)H_2$, $C(6)H_2^{asym}$	2958.4	−10.0	−7.8	1
CH_3^{asym}	2955.7	14.1	11.9		CH_3^{asym}	2955.7	13.0	10.9	
$C(5)H_2^{asym}$	2944.8	39.7	43.9	1,2	$C(5)H_2^{asym}$	2941.9	20.2	21.3	1
$C(4)H_2^{asym}$	2934.7	−31.2	−37.8	2	$C(5)H_2^{sym}$	2905.8	10.9	10.6	3
$C(5)H_2^{sym}$	2905.7	14.5	14.4	3	CH_3^{sym}	2904.5	0.5	0.8	
CH_3^{sym}	2904.5	−0.7	−0.6		$C(2)H_2$, $C(6)H_2^{sym}$	2901.6	−14.3	−18.1	3,4
$C(2)H_2$, $C(6)H_2^{sym}$	2901.6	−13.1	−17.0	3,4	$C(2)H_2$, $C(6)H_2^{sym}$	2900.5	−9.5	−7.1	3,4
$C(2)H_2$, $C(6)H_2^{sym}$	2900.5	−14.9	−12.6	3,4	C(3)H	2878.2	5.6	6.6	4
$C(4)H_2^{sym}$	2885.3	26.9	42.3	5	$C(4)D_2^{asym}$	2197.0			
C(3)H	2875.6	−10.9	−22.1	4,5	$C(4)D_2^{sym}$	2114.3			
	(+)MCH-*2,2,6,6-d*$_4$					(+)MCH-*5,5-d*$_2$			
CH_3^{asym}	2962.9	−1.0	−1.0	6	CH_3^{asym}	2962.9	3.5	1.7	
CH_3^{asym}	2955.8	4.0	3.5	6	$C(2)H_2$, $C(6)H_2^{asym}$	2960.8	−9.9	−6.5	
$C(5)H_2^{asym}$	2946.5	22.7	26.8	2	$C(2)H_2$, $C(6)H_2^{asym}$	2958.0	−1.5	−1.3	
$C(4)H_2^{asym}$	2934.9	−35.5	−42.2	2	CH_3^{asym}	2955.7	11.4	9.7	
$C(5)H_2^{sym}$	2904.6	10.5	14.8		$C(4)H_2^{asym}$	2937.3	−4.4	−5.2	
CH_3^{sym}	2904.4	−10.8	−15.6		CH_3^{sym}	2904.5	−0.5	−0.3	
$C(4)H_2^{sym}$	2885.7	24.1	39.7	5	$C(2)H_2$, $C(6)H_2^{sym}$	2902.7	−2.0	−3.5	4
C(3)H	2876.3	−14.3	−26.3	5	$C(2)H_2$, $C(6)H_2^{sym}$	2901.1	−6.4	−5.8	4
$C(2)D_2$, $C(6)D_2^{asym}$	2214.9				$C(4)H_2^{sym}$	2885.7	22.1	35.6	5
$C(2)D_2$, $C(6)D_2^{asym}$	2207.6				C(3)H	2875.7	−12.3	−24.3	4,5
$C(2)D_2$, $C(6)D_2^{sym}$	2125.0				$C(5)D_2^{asym}$	2200.8			
$C(2)D_2$, $C(6)D_2^{sym}$	2121.6				$C(5)D_2^{sym}$	2127.3			
	(+)MCH-*methyl-d*$_3$					(+)MCH-*3-d*$_1$			
$C(2)H_2$, $C(6)H_2^{asym}$	2962.3	−13.2	−13.4	1	CH_3^{asym}	2962.9	−0.3	−0.3	
$C(2)H_2$, $C(6)H_2^{asym}$	2958.3	−0.01	0.7	1	$C(2)H_2$, $C(6)H_2^{asym}$	2962.2	−14.2	−14.2	1
$C(5)H_2^{asym}$	2944.8	43.2	47.2	1,2	$C(2)H_2$, $C(6)H_2^{asym}$	2957.9	−3.7	−2.9	1
$C(4)H_2^{asym}$	2934.8	−31.9	−38.7	2	CH_3^{asym}	2955.3	3.8	3.0	
$C(5)H_2^{sym}$	2905.7	13.8	13.4	3	$C(5)H_2^{asym}$	2944.6	44.9	50.2	1,2
$C(2)H_2$, $C(6)H_2^{sym}$	2901.6	−11.1	−14.8	3,4	$C(4)H_2^{asym}$	2934.4	−31.4	−38.6	2
$C(2)H_2$, $C(6)H_2^{sym}$	2900.5	−14.9	−12.8	3,4	$C(5)H_2^{sym}$	2905.7	14.5	14.4	3
$C(4)H_2^{sym}$	2885.5	23.9	39.8	5	CH_3^{sym}	2904.4	−1.1	−1.3	
C(3)H	2876.0	−9.8	−21.3	4,5	$C(2)H_2$, $C(6)H_2^{sym}$	2901.2	−7.4	−8.3	3
CD_3^{asym}	2208.7				$C(2)H_2$, $C(6)H_2^{sym}$	2900.3	−10.6	−9.5	3
CD_3^{asym}	2187.0				$C(4)H_2^{sym}$	2883.5	5.4	7.7	
CD_3^{sym}	2074.4				C(3)D	2136.2			

[a] Diagonal force constants (mdyn/Å): 4.680 [C(2)H, C(6)H)]; 4.655 (C(5)H); 4.610 (C(4)H); 4.510 (C(3)H); 4.720 (C(me)H). Interaction force constants: 0.020 [C(2)H–C(2)H and C(6)H–C(6)H]; 0.050 (C(5)H–C(5)H); 0.025 (C(4)H–C(4)H); 0.065 (C(me)H–C(me)H); 0.010 (CH–CH(trans)). [b] Primary motion in mode. [c] Rotational strength, 10^{-44} esu^2 cm^2, fixed partial charge model. [d] Rotational strength, 10^{-44} esu^2 cm^2, atomic polar tensor model. [e] Couplet numbers refer to assignment in Table VI.

Fermi resonance analysis. Although each calculated normal mode has a dominant contribution from one or two localized internal symmetry coordinates, contributions from CH oscillation on adjacent carbon centers are present in all modes even in the absence of interaction force constants connecting the bond stretches, due to kinetic energy coupling. Adding a small positive CH,CH interaction force constant for trans CH bonds increases the mixing but does not alter the relative phasings of the CH motions in each normal mode. This interaction force constant also increases the calculated splitting between the two antisymmetric or two symmetric modes localized at C(2) and C(6). The CH stretching frequency shifts observed among isotopic samples also suggest that there is some small potential energy coupling between CH groups on adjacent carbons.

We have used the calculated atomic displacements to determine the dipole and rotational strengths for the CH stretching modes with the fixed partial charge[9] (FPC) and atomic polar tensor (APT)[31] models of VCD. For the FPC calculations, partial charges were set equal to +0.0346e for hydrogens on C(2) and C(6), 0.173e for all other hydrogens, and −0.3145e for oxygen, keeping the C=O and CH_n groups neutral. Other choices of partial charges, such as those employed previously by Singh and Keiderling[12] and Marcott et al.,[11] give similar results. The APT calculations were carried out with CNDO wave functions as previously described.[31] This model does not require empirical parameters and includes the effects of local charge flow.

The calculated frequencies, mode descriptions, and FPC and APT rotational strengths are presented in Table V for the six isotopomers. The APT rotational strengths are quite similar to those determined from the FPC model for all isotopomers. In comparing the tabulated calculated intensities to the experimental VCD spectra in Figure 2a–e, the Fermi resonances must be considered; that is, both absorption and VCD intensity for each unperturbed symmetric stretch is partitioned among the perturbed modes in proportion to the contribution from the fundamental with the approximation that the electric and magnetic dipole transition moments for the unperturbed overtone are negligible. For the strongly perturbed modes, the fundamental has nearly equal contributions to each component. The calculated VCD patterns for the FPC and APT models agree well with experiment for all the chiral isotopomers of 3-methylcyclohexanone, with the exception of the VCD due to the methyl symmetric stretch.

Coupled Oscillator Interpretation

To gain further insight into the mechanism producing the VCD features, and to enable us to readily interpret the VCD spectra of similar molecules, we have analyzed the VCD spectra of (+)-MCH in terms of the superposition of contributions from coupled oscillators on adjacent carbon atoms. We consider six types of coupling shown in Figure 5. The normal coordinate calculations show that the two adjacent motions are always found to couple such that the trans CH bonds vibrate in-phase (both are contracting or elongating) in the higher frequency mode and

(31) Freedman, T. B.; Nafie, L. A. *J. Phys. Chem.* **1984**, *88*, 496.

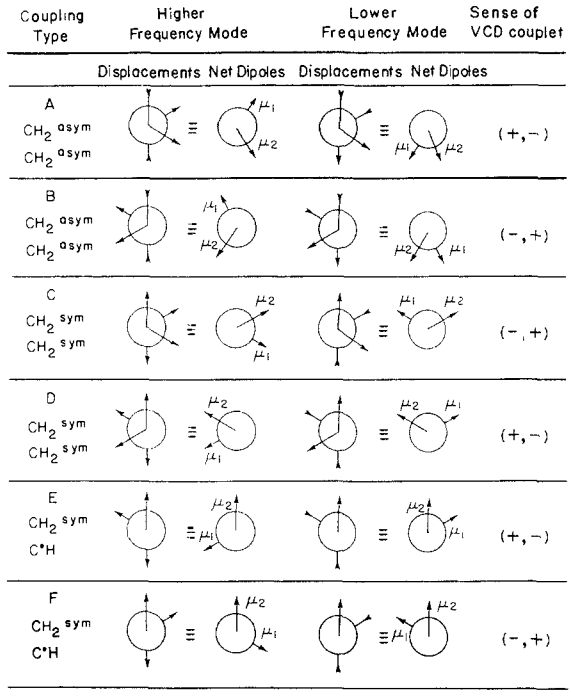

Figure 5. VCD couplets arising from coupled CH strecthing motions on adjacent carbon centers. For each member of a couplet, the arrows on the Newman projection to the left indicate the relative bond displacements (elongation or contraction) and the arrows on the Newman projection to the right show the relative orientation of the net electric dipole transition moments for oscillators localized at each carbon center.

out-of-phase (one trans CH bond is elongating and the other contracting) in the lower frequency mode. In the Newman projections in Figure 5 we show both the relative directions of the CH displacements and the relative directions of the resultant local electric dipole moment derivatives. The sign of the rotational strength is determined from the direction of these dipoles by[7]

$$R_{01} \propto -T_{12}\cdot(\mu_1 \times \mu_2)$$

where T_{12} is a separation vector directed from dipole μ_1 to dipole μ_2 in the Newman projection.

From the displacement vectors calculated for each normal mode of (+)-MCH we can identify five coupled oscillators of the types shown in Figure 5 that superimpose to form the VCD spectra. In addition, a sixth couplet due to the removal of the degeneracy in the methyl antisymmetric stretches by the chiral environment is also present. The couplets are listed in Table VI for the unperturbed CH stretching modes.

In the VCD spectrum of (+)-3-MCH, Figure 2a, we find that the negative 2960 cm^{-1} feature arises from the higher frequency components of both couplets 1 and 6. The positive shoulder at 2951 cm^{-1} is the second component of couplet 6. The strong positive feature at 2945 cm^{-1} arises from the coupling of the $C(5)H_2$ antisymmetric stretch with both the $C(6)H_2$ antisymmetric stretch (couplet 1) and the $C(4)H_2$ antisymmetric stretch (couplet 2). The second component of couplet 2 produces the negative lobe observed at ~2930 cm^{-1}. The shoulder at 2923 cm^{-1} arises from overlap of the Fermi shifted positive lobe of couplet 3 and Fermi shifted negative lobe of couplet 3. The 2909 cm^{-1} positive feature is the Fermi perturbed positive lobe of couplet 5. The negative feature at 2892 cm^{-1} arises from couplet 4. The weak negative feature at ~2870 cm^{-1} is a super position of the intense negative lobe of couplet 5, and weaker positive contributions from couplet 4 and from Fermi perturbed couplet 3.

We now consider the effects of deuteriation. In (+)-MCH-*2,2,6,6-d*$_4$ (Figure 2b) couplets 1, 3, and 4 are absent, which results in VCD intensity decreases at 2962 and 2945 cm^{-1} (allowing the 2960 cm^{-1}, 2950 cm^{-1} couplet due to the methyl group modes to be distinguished) and the elmination of negative intensity at 2895 cm^{-1}. The large increase in negative intensity at 2875 cm^{-1} can be attributed in part to elimination of the positive contribution of couplet 4 at that frequency and in part to the elimination of the Fermi perturbed positive lobe of couplet 3. There is also some evidence that the symmetric methyl stretch exhibits positive VCD not reflected in the FPC calculations, since the VCD intensity at 2923 cm^{-1} in (+)-MCH-*2,2,6,6-d*$_4$ can no longer be due to couplet 3. As noted above, a component of the Fermi perturbed CH_3 symmetric stretch occurs at ~2927 cm^{-1}.

Table VI. CH Stretching VCD Couplets in 3(*R*)-Methylcyclohexanone

couplet no.	coupled modes	unperturbed freq	couplet type	comments
1	$C(5)H_2^{asym}$	2962, 2958 (−)	B	absent in
	± $C(6)H_2^{asym}$	2945 (+)		*2,2,6,6-d*$_4$; *5,5-d*$_2$
2	$C(4)H_2^{asym}$	2945 (+)	A	absent in
	± $C(5)H_2^{asym}$	2935 (−)		*4,4-d*$_2$; *5,5-d*$_2$
3	$C(5)H_2^{sym}$	2905 (+)	D	absent in
	± $C(6)H_2^{sym}$	2902, 2900 (−)		*2,2,6,6-d*$_4$; *5,5-d*$_2$
4	$C(2)H_2^{sym}$	2902, 2900 (−)	F	absent in
	± C(3)H	2876 (+)		*2,2,6,6-d*$_4$; *3-d*$_1$
5	$C(4)H_2^{sym}$	2885 (+)	E	absent in
	± C(3)H	2876 (−)		*4,4-d*$_2$; *3-d*$_1$
6	CH_3^{asym}	2962 (−)	methyl	absent in
	CH_3^{asym}	2956 (+)		*methyl-d*$_3$

Deuteriation of the methyl group (Figure 2c) eliminates the contribution of couplet 6 at 2965, 2956 cm^{-1}. The net VCD due to couplet 3 is evident at 2925 cm^{-1}, without interference from the symmetric CH_3 stretch. The relative intensity alterations in the remaining modes compared to (+)-MCH reflect some mixing of methyl motion into many predominantly methylene modes.

In (+)MCH-*4,4-d*$_2$, couplets 2 and 5 are eliminated. In Figure 2d there is now clear evidence of couplet 1 (2963 cm^{-1} (−) and 2945 cm^{-1} (+)) and couplet 4 (2898 cm^{-1} (−) and 2877 cm^{-1} (+)). The negative VCD intensity at 2918 cm^{-1} derives from the Fermi shifted negative lobe of couplet 3; the positive Fermi shifted lobe of couplet 3 appears to broaden the lower frequency side of the 2945 cm^{-1} positive VCD band. Some of the positive VCD at 2877 cm^{-1} can also be attributed to the second Fermi component of the positive lobe of couplet 3.

Although the data in Figure 2e for (+)MCH-*5,5-d*$_2$ are less certain since the base line was extrapolated, the general VCD pattern is consistent with the above interpretations for the other isotopomers. The characteristic (+,−) couplet 2 is absent as expected. The positive VCD at 2907 cm^{-1} and broad negative VCD at ~2890 and 2870 cm^{-1} are attributed to a superposition of couplets 4 and 5. Positive VCD due to the methyl group symmetric stretch is clearly evident at ~2935 cm^{-1}, since both couplets 2 and 3 are absent. Finally, the mixed $C(6)H_2$, $C(2)H_2$, and methyl antisymmetric stretching modes yield net positive VCD producing the highest frequency lobe, as predicted from the FPC calculation, but not readily determined from simple coupled oscillator considerations.

The couplets identified here are also evident in the FPC calculations in Table V, as we have indicated in the table. The calculations also include the effects of mixing of non-adjacent CH stretching motion, particularly important for accidently degenerate modes such as the antisymmetric methyl and antisymmetric $C(2)H_2$, $C(6)H_2$ modes. These effects tend to cancel in the observed spectra.

In contrast to the CH stretching VCD, the VCD spectrum in the CD stretching region of (+)MCH-*2,2,6,6-d*$_4$ does not follow the pattern expected from the coupled oscillator mechanism, i.e., weak nearly conservative couplets for the split symmetric or antisymmetric modes. Such couplets would arise from the mixing of A′ and A″ α-CD_2 stretching modes in cyclohexanone-*2,2,6,6-d*$_4$ due to lowering the symmetry by adding the 3-methyl group in forming 3-methylcyclohexanone. The observed spectra (Figure 2f) in fact consist of a dominant negative feature corresponding to the higher frequency antisymmetric CD stretch, and weak positive VCD spread out among the remaining modes. The negatively biased VCD in this region is indicative of the ring current mechanism of VCD. It is conceivable that the concerted out-of-phase motion of the equatorial C(2)H and C(6)H bonds

could initiate current flow through the carbonyl carbon. The asymmetry of the molecule should introduce a component of the electric dipole transition moment μ for this mode that is orthogonal to the projected ring plane, resulting in ring current enhancement. In the CH stretching region the small VCD contribution due to this mechanism is not apparent due to the strong mixing among the local vibrations.

Discussion

We conclude from our analysis that the coupled oscillator mechanism is the predominant source of VCD intensity in the CH stretching region of (+)-3(*R*)-methylcyclohexanone and its deuteriated isotopomers. This analysis can be readily applied to similar chiral molecules. From knowledge of the predominant local motion generating each vibrational band and the molecular conformation, the VCD pattern can be predicted by considering the coupling of CH stretching modes on adjacent carbon centers. Since the local motions mix such that the higher frequency coupled mode always involves the in-plane motion of trans CH bonds, the sense of each couplet can be readily determined from the molecular geometry by means of the coupled oscillator mechanism. Conversely, if the vibrational assignments are known, the local conformation can be deduced from the sense of the observed VCD couplets. Since the antisymmetric methylene stretches are less perturbed by Fermi resonance, the region above $\sim$2930 cm^{-1} provides a more consistent probe of molecular structure, since the bands are more readily assigned.

The origin of the characteristic VCD pattern for the chiral $CH_2CH_2C^*H$ fragment reported by Laux et al.[20,21] is now clear. The higher frequency (+,–) couplet for the fragment in conformation **1** arises from couplet type A (Figure 5) for the antisymmetric stretches of the two methylenes in the fragment. In conformation **2**, these modes generate couplet type B, a (–,+) couplets arising from the mirror image of the motions in couplet A. The sense of the VCD couplet depends only on the phasing of the adjacent CH_2 stretching contributions in each mode, independent of which methylene has the larger contribution to a mode. The third, lowest frequency positive VCD component characteristic of the fragment in conformation **1** is largely the positive lobe of couplet type E due to coupling of the methine stretch to the symmetric stretch of the adjacent methylene in the fragment, which is displaced to higher frequency by Fermi resonance. Closer scrutiny of the spectra recorded by Laux reveals that the negative lobe of the type E couplet is indeed present at $\sim$2870–2860 cm^{-1} for most of the compounds in conformation **1**.[21] These include *R*-(+)-3-*tert*-butylcyclohexanone, (–)-menthone, (+)-limonene, (+)-*p*-menth-1-ene, (+)-*p*-menth-1-en-9-ol, (+)-pulegone, and (–)-menthol. For this couplet, the mode that is predominantly methylene symmetric stretch must be at a higher frequency than the methine stretch in the absence of Fermi resonance in each of these molecules, since the positive lobe of the couplet is shifted to 2900 cm^{-1} or above by the Fermi resonance. The low methine stretching frequency, $\sim$2870 cm^{-1}, implies a considerably lower force constant for the methine CH bond, compared to a methyl or methylene CH.

For the fragment in conformation **2**, a methylene symmetric stretch/methine stretch couplet (E or F) is not present, since the two adjacent modes have nearly parallel or antiparallel electric dipole transition moments in this conformation. The lower frequency VCD bands in (–)-β-pinene and (–)-*cis*-myratanylamine, $\sim$2923 cm^{-1}, which were attributed to the chiral fragment,[20,21] may in fact arise from other modes in these molecules, such as the symmetric stretch of a bridgehead methyl group. In 3-methylcyclohexanone we find that the VCD band at $\sim$2920 cm^{-1} in fact involves three or more fundamentals, including contributions from methine, methyl, and methylene motions.

The VCD contributions from the methyl group, particularly the symmetric methyl stretch, are not well described by the FPC calculations or descriptive coupled oscillator considerations. The methyl VCD intensity arises from the chiral environment of the group, which both removes the degeneracy in the antisymmetric stretches and mixes the symmetric and antisymmetric motions. Insufficient data are available from the spectra to describe adequately the chiral perturbation and force field for the methyl group in 3(*R*)-methylcyclohexanone. In contrast, two adjacent methylene groups or a methylene and adjacent methine form a chiral structure for which the coupled, chiral vibrations are readily determined. The methylene and methine modes are thus a more valuable probe of local conformation than are the methyl modes.

Finally, we emphasize the importance of considering Fermi resonance interactions when interpreting both absorption and VCD spectra in the CH stretching region. We found it sufficient to consider only local group resonances in order to estimate the frequencies of unperturbed fundamentals. For two coupled modes that can both interact with a single overtone, the perturbed modes will have varying VCD contributions of opposite sign from the two fundamentals. Such mixing may reduce the VCD intensity of the perturbed modes and may account for the broad negative VCD noted for the region below $\sim$2860 cm^{-1} in some of the isotopomers.

Acknowledgment. The authors acknowledge the National Science Foundation (CHE 86-02854) and the National Institutes of Health (GM-23567) for financial support. We thank Drs. Anita Chernovitz, William Zuk, and Carl Zimba for recording some of the spectra reported here.